CrossMark

ORIGINAL RESEARCH

Post-treatment sludge analyses and purification of paint effluent by coag-flocculation method

M. C. Menkiti[1,2] · I. G. Ezemagu[2] · C. I. Nwoye[3] · M. I. Ejimofor[2]

Abstract *Tympanotonos fuscatus* shell (*T. fuscatus* shell), an abundant eco-friendly waste was used as a precursor for the production of *Tympanotonos fuscatus* coagulant (TFC) for the purification of paint effluent (PE). *Tympanotonos fuscatus* shells (TFS) are of crustacean origin consisting mainly of chitin, calcium carbonate, entrained protein and other organic matrixes. Influence of pH, dosage and settling time on treatment efficiency was studied. Scanning electron microscopic, Fourier transform infra red, X-ray diffraction and differential scanning calorimetric/thermogravimetric analyses were carried out to investigate, respectively, the surface morphology, functional group, crystalline/lattice structure and thermal stability of TFS, TFC and settled sludge after treatment. The PE was optimally treated at 2 g/L TFC dosage, pH 5 and 97 % efficiency. Results indicated that TFC could be an efficient treatment agent for PE at the conditions of the experiment.

✉ M. C. Menkiti
cmenkiti@yahoo.com; matthew.menkiti@ttu.edu

I. G. Ezemagu
ifegodfey@yahoo.co.uk

C. I. Nwoye
nwoyennike@gmail.com

M. I. Ejimofor
ejohmarc@gmail.com

1   Civil and Environmental Engineering, Water Resources Center, Texas Tech University, Lubbock, TX, USA

2   Department of Chemical Engineering, Nnamdi Azikiwe University, Awka, Nigeria

3   Department of Materials and Metallurgical Engineering, Nnamdi Azikiwe University, Awka, Nigeria

Abbreviations

K_B	Boltzmann's constant
K_m	Menkonu coag-flocculation rate constant
K_R	Von Smoluchowski coag-flocculation constant
β_{BR}	Collision factor for Brownian transport
ε_p	Collision efficiency
$\tau_{1/2}$	Coagulation period/half life
E	Coag-flocculation efficiency
R^2	Coefficient of determination
$á$	Coag-flocculation reaction order
$-r$	Coag-flocculation reaction rate
T	Absolute temperature
TFC	*Tympanotonos fuscatus* coagulant
TFS	*Tympanotonos fuscatus* shell
TSS	Total suspended solid
TDS	Total dissolved solid
TS	Total solid
SSAT	Settled sludge after treatment
SD	Standard deviation
PE	Paint effluent
RMSE	Root mean square error
SSE	Sum of square error
RE	Relative error
N_0	Concentration of turbidity at time $t = 0$
N_t	Concentration of turbidity at time

Introduction

Paint production is one of the small- and medium-scale enterprises (SME) in Nigeria. Along the production line, hazardous and turbid paint effluent (PE) is generated. The paint effluent generated in the course of production would be toxic and bears suspended particles, odor and color [1].

Hence, the need to treat paint effluent to meet Nigeria National Environment (standards for discharge of effluent into water or on land) Regulations standard before discharging to the environment becomes imperative.

Several treatment methods are applied in wastewater treatment, such as adsorption, oxidation process, lime addition, neutralization, membrane filtration, ion exchange, reverse osmosis and coag-flocculation [2].

Among these methods, coag-flocculation using eco-friendly biomaterials present a more viable treatment alternative for initial purification of paint effluent. The advantages of coag-flocculation over other methods include: (1) its simplicity and less energy demand, (2) low cost and (3) reliably robust and efficient [3, 4].

Coagulation is a process of destabilizing particles by a coagulant to promote aggregation by Brownian motion due to action of shear forces [5]. Factors such as pH, quality of raw effluent, nature of effluent and temperature influence coag-flocculation [6].

Fundamentally, chemical coagulants such as ferric chloride, ferric sulfate, ferrous sulfate, alum, polyaluminum and lime have been widely used to coagulate industrial effluents [2]. However, these traditional coagulants have several disadvantages, which include: large volume of sludge [7]; dissolution of metals/constituents into after treatment sludge, under performance and corrosiveness at lower pH and pKa (dissociation constant of a solution) [8]. In addition, Miller et al. [9] and Crapper et al. [10], reported that these alum-based chemical coagulants can cause pre-senile dementia in human.

These disadvantages underscore the need for alternative, cost-effective and environmentally friendly substitutes to mineral coagulants, in view of global demand for the consideration of eco-friendly biomaterials. Eco-friendly bio-coagulants are essentially presumed safe for environmental and human health. Being extracts from plants and animals, they are biodegradable and unlikely to produce treated water with extreme pH [11]. In the age of ozone layer depletion, climate change and widespread environmental degradation, application of these eco-friendly biomaterials in purification of paint effluent is desirable in other to sustain safe global environmental initiatives. Biomaterials such as Nirmali seed [12]; okra [13]; *mucuna* seed [14]; red bean, sugar and red maize [15]; and *Tympanotonos fuscatus* shell (TFS) have been identified as coagulants, with the later being the focus of this report.

TFS (images shown in Fig. 1) [16] is composed of natural chitin, which is a major component of the shells of crustacean [17, 18]. Other components of TFS are calcium carbonate, entrained protein and color pigment. In addition, TFS can also be used for construction and as a source of animal feed [19]. On deacetylation of TFS, it converts to chitosan that constitutes the active coagulation ingredient [11]. TFS are

Fig. 1 Images of TFS

huge solid waste in Nigeria and constitute environmental pollutant in producing zones. The utilization of the shells would put this waste to useful ends while also promoting a cleaner environment. The waste shells are obtained after separating the edible flesh from the shells. In this study, the non-food competing TFS had been used as a precursor for the production of TFC, which has been previously subjected to novel trials for the purification of coal washery effluent [20]. Progress made in the previous application necessitated its trial on the purification of PE, which currently constitutes hazard to the environment. Specifically, there is no existing study on the basic characteristics of after treatment sludge generated from biocoagulation of PE using natural extracts. Previous sludge study had generally been on sludge generated from the use of mineral coagulants [21], which could hardly be put to further use due to harmful nature of the mineral coagulants contained in the sludge. To advance the use of SSAT (of bio-extracts), this exploratory study endeavored to give insight into its basic characteristics, its likely further useful potential application and disposal options available to ensure green environment. This current study would close the gaps on previous and current studies that had investigated effluent treatment process without inclusion of basic study on after treatment sludge.

In this work, therefore, the major objectives include focus on the potential application of TFC on treatment of PE to reduce its turbidity, in addition to the evaluation of the effects of process variables. The coagulation kinetics was also studied as well as chemical and instrumental

characterization of TFS, TFC and settled sludge after treatment (SSAT). Statistical analyses of the experimental results were also conducted.

Materials and methods

Material collection

Paint effluent (PE)

The paint effluent for the studies was obtained from a factory at Onitsha, Anambra State, Nigeria. The effluent was stored in a black plastic container to prevent changes in the characteristics of the effluent.

TFS and TFC

TFS used were sourced from Onitsha, Nigeria. It was thoroughly washed, dried, ground and sieved with 0.5 mm standard sieve to obtain an amount stored in desiccators and further processed to TFC.

In processing TFS to TFC, deproteinization of ground TFS sample was firstly done by agitating continuously 0.5 L of 1 M NaOH solution containing 50 g powdered TFS for 2 h at 70 °C. On cooling, the mixture was separated and resulting solid sample was washed using distilled water for 30 min and subsequently dried (at 70 °C for 2 h) using oven. The deproteinized powdered TFS was demineralized for 30 min in a constantly stirred 0.25 L–1 M HCl solution, and the resulting TFS-HCl mixture separated by filter paper. The resulting solid residue was washed thoroughly using distilled water for 30 min and followed by oven drying at 70 °C for 2 h. The ground TFS obtained after demineralization was deacetylated using autoclave (at 15 psi) for 30 min at 122 °C using 50 % concentrated NaOH solution, applied at 1:10 (w/v) solid to solution ratio. The sample produced after autoclaving was washed to pH 7 using running distilled water and subsequently oven dried for 2 h at 70 °C. This processed end product of ground TFS was termed TFC.

Material characterization

Analysis of physical properties of PE

The wastewater characterization was based on American Public Health Association (APHA) procedures [22].

Analysis of physiochemical properties of TFC

Percentage yield/weight loss   90 g of TFS was weighed and processed to TFC of weight A. Thus,

$$\text{Percentage yield} = \frac{A}{90} \times 100 \qquad (1)$$

$$\text{Percentage weight loss} = \frac{90 - A}{90} \times 100. \qquad (2)$$

Bulk density   W weight of TFS was used to fill up a container of 1000 mL. Thus,

$$\text{Bulk density} = \frac{W}{V} \qquad (3)$$

where W is weight of the TFS and V is volume of the container.

Percentage ash content   4 g of the dried TFS was burnt in a muffle furnace at 600 °C to yield gray-white residue. Thus,

$$\text{Ash content } (\%) = \frac{W_{\text{ash}}}{W_{\text{sample}}} \times 100 \qquad (4)$$

where W_{ash} is weight of ash and W_{sample} is weight of TFS sample.

Percentage oil content   20 g of powdered TFS was wrapped in a filter paper and placed in a Soxhlet extractor attached to a round bottom flask containing 150 mL of hexane. Heat was applied to the set up and extraction is considered complete when the extracting solution becomes clear. The extract (oil) was left for 7 days to evaporate entrained solvent. Thus,

$$\% \text{ Oil yield} = \frac{W_{\text{oil}}}{W_{\text{sample}}} \times 100 \qquad (5)$$

where W_{oil} is the weight of oil and W_{sample} is the weight of sample.

Percentage moisture content   2 g of TFS was heated in oven at 160 °C for 6 h and measured to a constant weight. Thus,

$$\% \text{ Moisture content} = \frac{W_{\text{sample}} - W_{\text{dry}}}{W_{\text{sample}}} \times 100 \qquad (6)$$

where W_{sample} is the weight of precursor before drying, W_{dry} is weight of precursor after drying.

Percentage protein content   2 g of TFS flour was put into a Kjeldahl digestion flask containing 8 g of catalyst (96 % anhydrous Na_2SO_4, 3.5 % $CuSO_4 \cdot 5H_2O$, 0.5 % Selenium dioxide). 10.1 mL of conc. H_2SO_4 was added to the flask and shaken occasionally for 2 h. 50 mL of boric acid solution (2 %) and screened methyl red indicator were added to the flask after cooling. The apparatus was connected with the delivery tube deepened below the boric acid solution. 50 % NaOH solution was added to alkalize

the digest. 50 mL each of the distillate and a blank were titrated under same conditions using 0.1 M H2SO4. Thus,

$$\% \text{ Nitrogen} = \text{volume of } 0.1 \text{ M H}_2\text{SO}_4 \tag{7}$$

$$\text{Protein content} = \% \text{ nitrogen} \times 6.25 \tag{8}$$

Instrumental characterization of TFS, TF and SSAT The surface morphology, functional groups and lattice/crystalline structure of the samples were determined using model Zeiss Evo®MA 15 EDX/WDS microscope, Model 470/670/870 Thermo Nicolet Nexus unit and PHILIPS X PERT X-RAY unit, respectively. Thermal characteristics of samples were analyzed using models TGA-Q50 and DSC-Q200 units.

Coag-flocculation factors impact

Influence of TFC dosage variation

1. Native pH and initial particle load on the paint effluent (PE) were measured at ambient temperature.
2. Samples of 1000 mL of PE in ten different 1000-mL beakers were fed with 0.5–5 g/L *Tympanotonos fuscatus* coagulant (TFC).
3. The PE/TFC in the 1000-mL beakers were firstly subjected to rapid mixing (110 rpm for 2 min) and followed by slow mixing (35 rpm for 20 min). At the expiration of slow mixing, the PE/TFC supernatants were brought down and allowed to stand for 30 min.
4. At 30 min, 15 mL of the supernatant was taken at 2 cm depth from each of the beakers and drained into cuvettes.
5. The residual turbidity of supernatants was determined. Particle concentration was calculated as a product of turbidity (NTU) and T_f. T_f is a conversion factor that converts turbidity to particle concentration. T_f has a value of 2.35 [23].

Influence of PE pH variation

1. Samples of optimum dosage from "Influence of TFC dosage variation" were charged into 8 beakers containing 1000 mL of PE each. Native pH 8 of PE was adjusted from 2 to 9 using 0.1 M H2SO4 and 0.1 M NaOH prior to dosing.
2. Steps (3)–(5) of "Influence of TFC dosage variation" were repeated.

Influence of time on removal efficiency

1. Sample of optimum dosage was fed into 1000 mL PE.
2. Step (3) of "Influence of TFC dosage variation" was repeated. While settling, residual turbidity values were

recorded at 3–30 min based on "Influence of TFC dosage variation".

Coagulation kinetics theory

For the cases of monodisperse, no break up and biparticle collisions [24–26]:

$$\frac{dn_k}{dt} = \frac{1}{2}\sum_{i+j=k}\beta_{BR}(i,j)n_i n_j - \sum_{i=1}^{\infty}\beta_{BR}(i,k)n_i n_k \tag{9}$$

where $\frac{dnk}{dt}$ is the coag-flocculation rate. $\beta_{BR}(i,j)$ represents coag-flocculation transport mechanism. n_i and n_j are concentrations for particles of size i and j, respectively. β_{BR} [27] is defined by Eq. 10:

$$\beta_{BR} = \frac{8}{3}\varepsilon_P\frac{K_B T}{\eta} \tag{10}$$

where K_B is Boltzmann's constant (J/K), T is absolute temperature (K), ε_p is the collision efficiency, η is the viscosity of the fluid.

For rapid coagulation

$$K_R = 8\pi a D' \tag{11}$$

where K_R is the Von Smoluchowski rate constant for rapid coagulation [28], a is particle radius and D' is diffusion coefficient.

Equation 11 is simplified to

$$K_R = \frac{4}{3}\frac{K_B T}{\eta} \tag{12}$$

Equations 10–12 can be transformed to Eq. 13 [14]:

$$K_m = \frac{1}{2}\beta_{BR} \tag{13}$$

where K_m is Menkonu coagulation–flocculation rate constant. For Brownian aggregation, rate could also be [26, 29]:

$$-\frac{dN_t}{dt} = K_m N_t^{\alpha} \tag{14}$$

N_t is the total particle concentration at time t. Also, for rapid coag-flocculation $1 \le \alpha \le 2$ [30].

Thus,

$$\text{for } \alpha = 1 : \ln\left(\frac{1}{N}\right) = K_m t - \ln N_0 \tag{15}$$

$$\text{for } \alpha = 2 : \frac{1}{N} = K_m t + \frac{1}{N_0} \tag{16}$$

where N_0 is the initial N_t at time = 0. N is N_t at upper time limit >0. Plot of $\frac{1}{N}$ vs t produces a slope of K_m and intercept of $\frac{1}{N_0}$.

For coagulation period $\tau_{1/2}$ Eq. 16 yields Eq 17:

$$\tau_{1/2} = 1/(0.5N_0K_m). \tag{17}$$

Equation 18 gives coagulation–flocculation efficiency

$$E\ (\%) = \left[\frac{N_0 - N_t}{N_0}\right]100. \tag{18}$$

Statistical analyses

Standard deviation and the statistical error analyses were calculated using Eqs. 19–20 and 21–23, respectively; where A_v, SD, RMSE, SSE and RE are the average mean, standard deviation, root mean square error, sum of square error and relative error, respectively.

$$A_v = \sum \left(\frac{q_{i_{exp}}}{N_i}\right) \tag{19}$$

$$SD = \sqrt{\frac{1}{N_i}\sum (q_{i_{exp}} - A_v)^2} \tag{20}$$

$$RMSE = \sqrt{\frac{1}{N}\sum_{i=1}^{N}\left(\left(\frac{q_{i_{exp}} - q_{i_{cal}}}{q_{i_{exp}}}\right)^2\right)} \tag{21}$$

$$SSE = \sum (q_{i_{exp}} - q_{i_{cal}}) \tag{22}$$

$$RE = \frac{100}{N}\sum_{i=1}^{N}\left(\frac{q_{i_{exp}} - q_{i_{cal}}}{q_{i_{exp}}}\right) \tag{23}$$

where $q_{i_{exp}}$ and $q_{i_{cal}}$ are the obtained experimental and predicted data.

Results and discussion

Characterization results

Physiochemical characteristics

Table 1 shows the values for total suspended solids (TSS), total dissolved solids (TDS) and total solid (TS) that are significant for the application of coagulation.

Table 2 shows that the yield value (80 %) and protein content (17 %) are quite significant. Hence, TFS can be considered a suitable precursor.

SEM and elemental analyses of TFS, TFC and SSAT

Pairs of SEM images of TFS, TFC and SSAT are shown as Figs. 2a, b, 3a, b and 4a, b, respectively. Figure 2a shows image of a single, magnified, irregular-shaped particle surrounded with dark field void. Similar heavily compact particles distribution is observed in Fig. 2b. Figure 2b shows the structure of smooth and sparsely dispersed stick-like particles surrounded by completely cemented pores.

Table 1 Characterization of paint effluent (PE)

Parameter	Value	NESRA
TSS	2679 mg/L	100 mg/L
PH	8	5–8
TDS	1600 mg/L	1200 mg/L
TS	4279 mg/L	1300 mg/L

National Environment (standards for discharge of effluent into water or on land) Regulations, (NESRA) S.I. No 5/1999

Table 2 *Tympanotonos fuscatus* shell proximate analysis

| Parameter	Value
Yield (%)	80
Weight loss (%)	20
Bulk density (g/mL)	0.12
Ash content (%)	4.98
Oil content (%)	10
Moisture content (%)	4.5
Protein (%)	17.7

Figure 3a, b shows images of sponge-like structure with voided pores scattered evenly on the surface of the structure. The morphology is white field unlike the TFS. The presence of the voided pores in TFC allowed for the trapping of particles within the pores surfaces. Figure 4 shows the images of SSAT with filled pores due to the deposition of particles. The filling of the pores noted could be linked to results displayed in Table 3.

Table 3 indicates that Ti, Fe, Cu, Cl, Al were absent in *Tympanotonos fuscatus* shell (TFS) but maintained presence in TFC and settled sludge after treatment (SSAT). More quantities of Na, Mg, Al, Si, Cl and Ca were contained in TFC when compared to TFS. The decrease in K, Al and Cl could be linked to the use of the elements for the formation of salts that filled significant voids in TFC as shown in SSAT images. It could be taught that chlorine present in the paint effluent (PE) took active part in the formation of the salt [31, 32] and subsequent depletion of Na, K and Al.

FTIR spectra analysis of TFS, TFC and SSAT

Figure 5 shows that spectra of TFS, TFC and SSAT exhibit 30, 19 and 22 discernible peaks at frequency of 600–4000 cm^{-1} with a threshold of 0.44, 1.17 and 0.88, respectively [33]. In Fig. 3a, 3335 cm^{-1} (N–H stretching) depicts the presence of secondary amine, supporting the presence of protein in TFS. 2919 cm^{-1} denotes C–H stretching while 1652, 1646 and 1635 cm^{-1} denote C=C stretching and NH_2. Peaks at 1463, 1455 and 1447 cm^{-1} indicate the presence of N=N stretching. 1034–1082 cm^{-1}
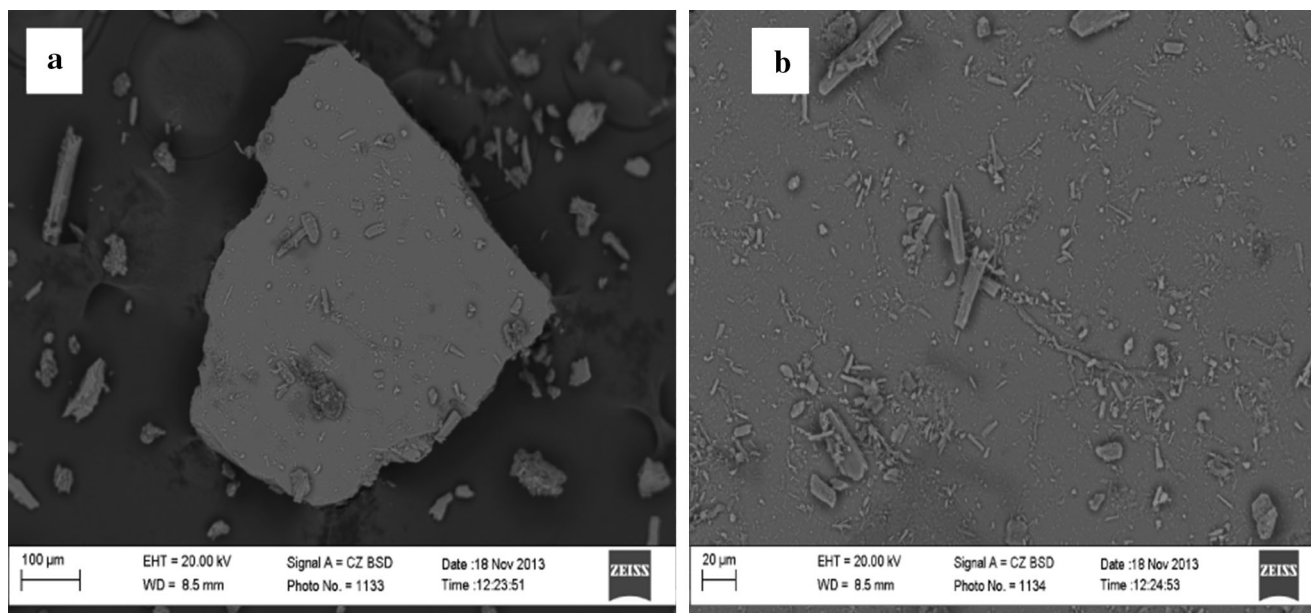
Fig. 2 SEM images of *Tympanotonos fuscatus* shell (TFS)
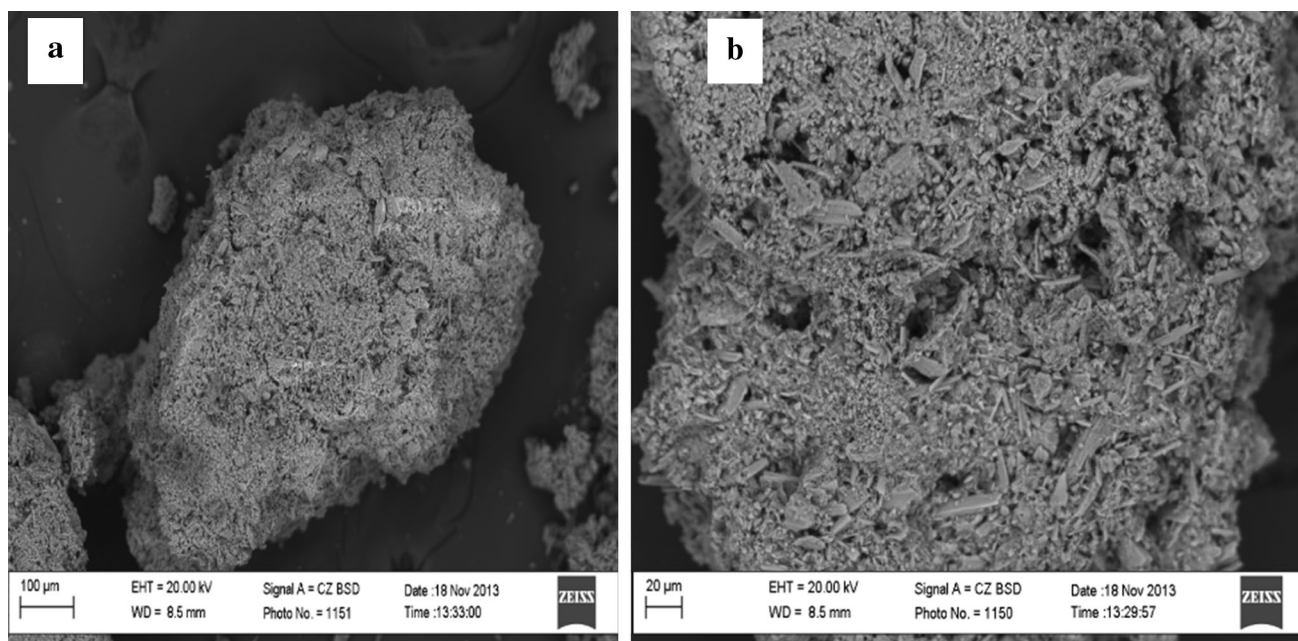
Fig. 3 SEM images of *Tympanotonos fuscatus* coagulant (TFC)

are characterized by C–O stretching. Peaks at 856, 712 and 700 cm^{-1} characterize NH$_2$ wagging and twisting, N–H wagging and =C–H bending, respectively. In Fig. 5b, peaks at 3850–3593 cm^{-1} (O–H stretching) are attributed to the presence of phenol and alcohol while band at 3296 cm^{-1}(N–H stretching) indicates the presence of

secondary amide groups. 2916 and 2850 cm^{-1} (methylene asymmetric and symmetric C–H stretching) indicate the presence of aliphatic hydrocarbon groups. For 1634 to 1443 cm^{-1}, C=C stretching, NH$_2$ scissoring, azo compound and N–H bending are indicated. Broad bands at 1082, 1068 and 1032 cm^{-1} indicate C–O stretching. Peaks
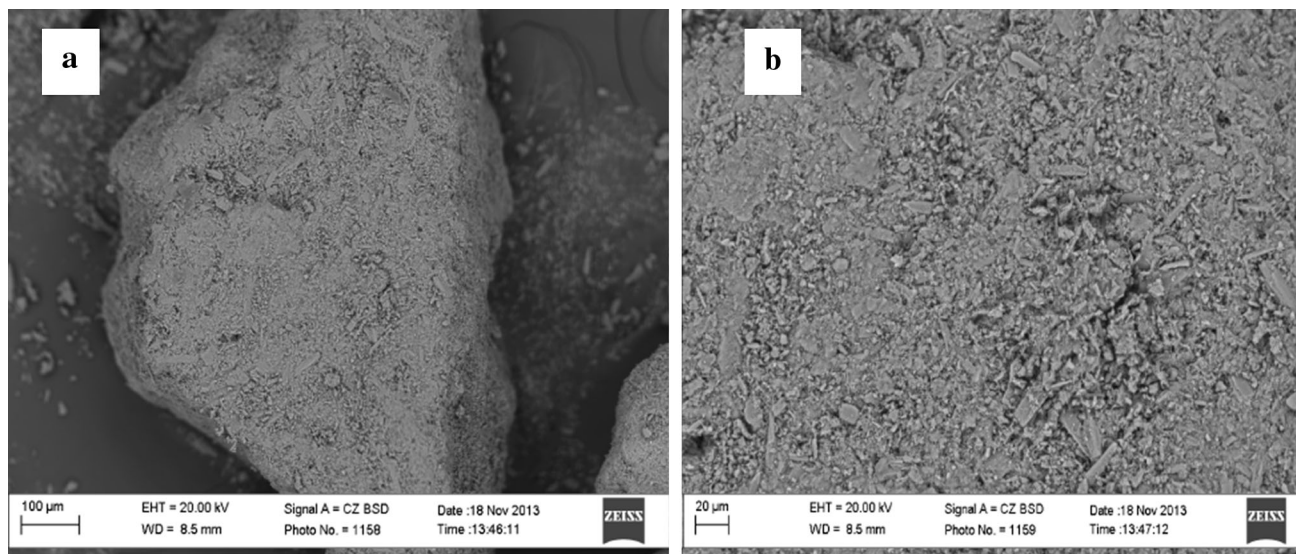
Fig. 4 SEM images of settled sludge after treatment (SSAT)

Table 3 Elemental composition of TFS, TFC and SSAT

| Element (Wt%)	TFS	TFC	SSAT
C	23.68	17.47	20.51
Na	0.99	31.65	5.14
Mg	0.68	3.18	18.63
Al	0.00	3.16	9.32
Si	0.00	4.49	11.49
P	0.00	0.00	0.00
S	0.00	0.00	0.00
Cl	0.00	0.81	0.49
K	0.00	0.19	0.00
Ca	195.77	153.69	127.17
Ti	0.00	0.00	8.38
Fe	0.00	1.91	5.51
Cu	0.00	0.00	0.00
O	78.93	83.07	93.36

at 909, 855, 781, 712 and 699 cm^{-1} (N–H stretching, NH$_2$ wagging and twisting, N–H wagging and =C–H bending) indicate the presence of amine and alkyne groups. Figure 5c shows distinct peaks at 1445 cm^{-1} (N=N stretching), 3335 cm^{-1} (N–H stretching), 2917, 2850 cm^{-1} (methylene symmetric and asymmetric of C–H stretching). Peaks at 1082, 1068, 1032 and 1009 cm^{-1} indicate the presence of esters, while 913, 857 cm^{-1} stand for N–H stretching and NH$_2$ wagging and twisting. The region of 712–699 cm^{-1} depicts the presence of alkyne group. Figure 5a–c showed that some peaks were shifted and also new peaks were detected.

XRD pattern of TFS, TFC and SSAT

Figure 6a–c shows 11 and 10 clear peaks, respectively. The peaks were assigned on the bases of their different reflections and planes. The left–right shifts might be linked to the expansion or contraction of the samples. The intense peaks for samples were caused by a small subset of crystallite in the powder that had a plane oriented exactly parallel to the reference plane. The system depicted 000 hkl for TFS, TFC and SSAT. This implies that the atomic structures of TFS, TFC and SSAT are of primitive crystalline structure.

### Differential scanning calorimetric (DSC) and thermogravimetric analyses (TGA) of TFS, TFC and SSAT

DSC and TGA indicate the thermal characteristics of samples [34–36] in Figs. 7–9. Figures 7a and 8a show the DSC profile for TFS and TFC over 37.5–296.875 °C and 37.5–297 °C, with enthalpy of 12.039 and 11.439 kJ/mol, respectively. The transition could be due to de-stringing and coiling of carbon chain resulting in spontaneous densification [37, 38]. Densification depicted in Figs. 7a and 8a, respectively, took place at 150–200 °C and 112.5–187.5 °C exothermically. The final residual mass for TFS (Fig. 7b) and TFC (Fig. 8b) was 3.259 mg and 3.520125 mg, representing 94.06 and 87.5 % of the original weights, respectively. The early and late weight losses in Figs. 7b and 8b were due to loss of internal moisture and labile component, respectively, from samples [37, 38].
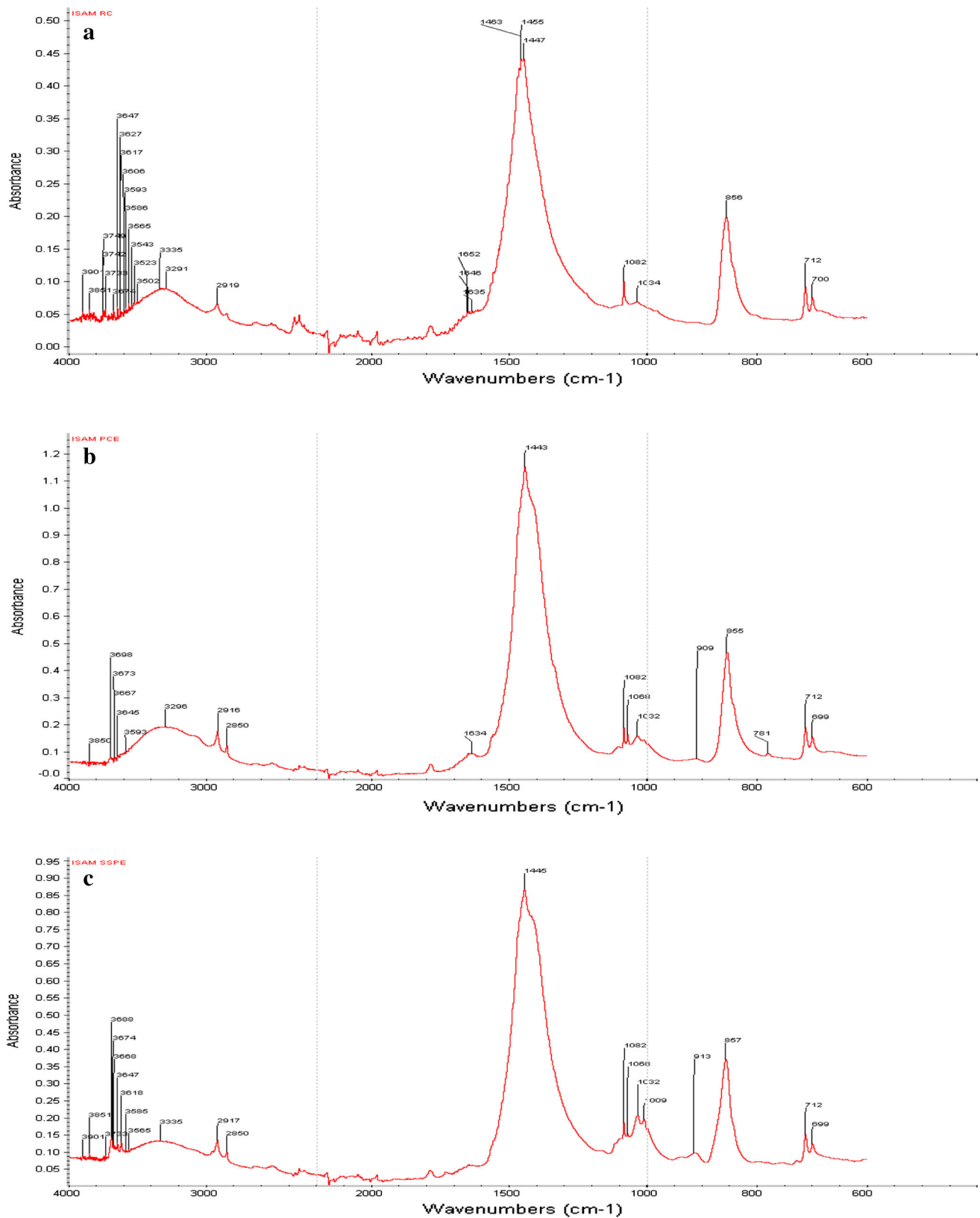
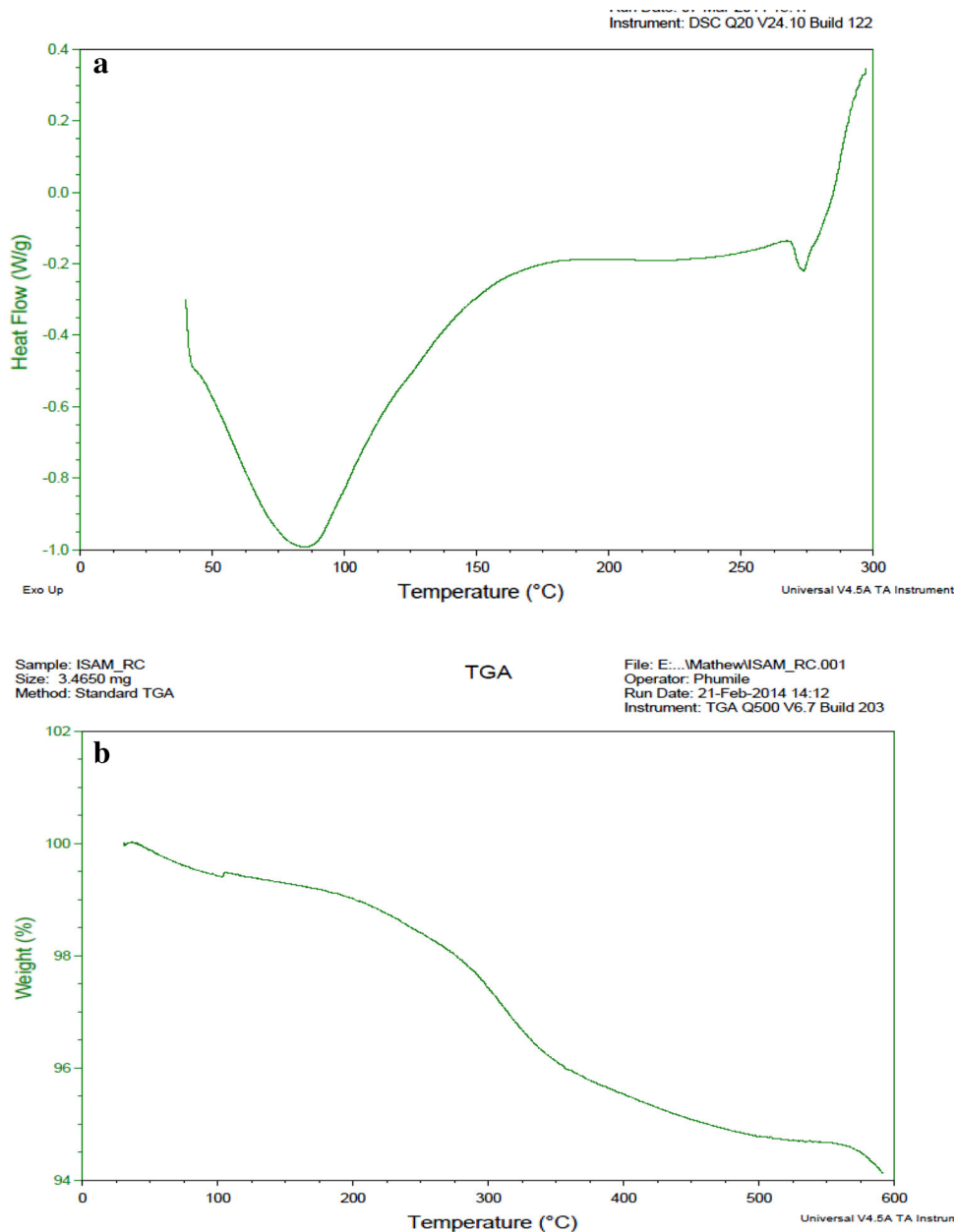Fig. 5 FTIR spectrum of: **a** TFS, **b** TFC and **c** settled sludge after treatment
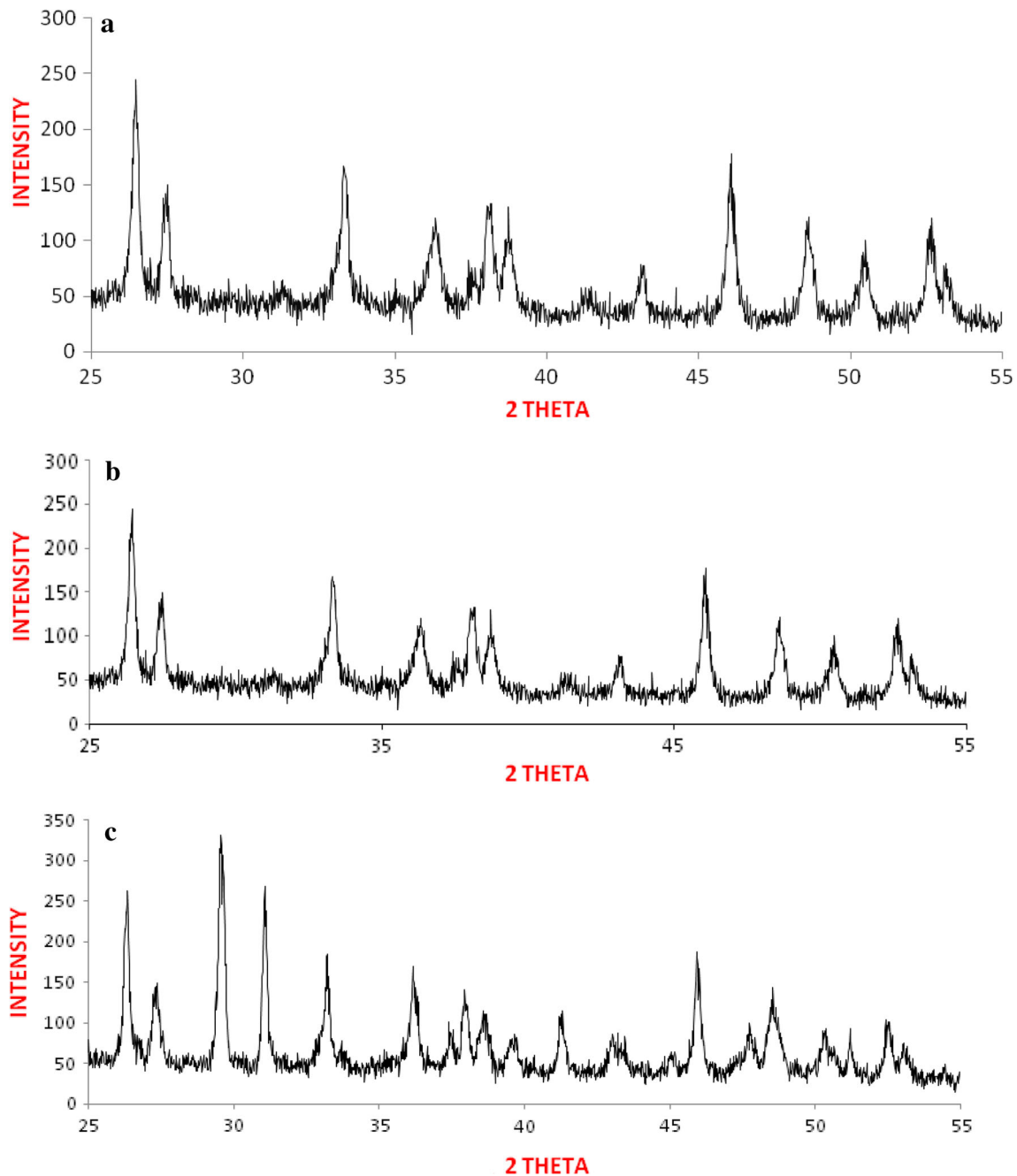
Fig. 6 XRD pattern for: **a** TFS, **b** TFC and **c** settled sludge after treatment

The eutectic points of SSAT due to inhomogeneous deposition of varying suspended and dissolved particles are depicted in Fig. 9a. Moreover, even though Fig. 9a indicates the presence of eutectic points, the process was still exothermic. Figure 9b indicates dehydration and volatilization of the samples mass at 310.5 °C, in which about 5 % (0.11985 mg) of its weight was lost [39]. On oxidization, about 10 % (0.2397 mg) of sample weight was lost between 310.5 and 462.5 °C. At 587.5 °C, 0.2996 mg was lost. Figure 9b shows maximum mass loss of 15 % (0.2996 mg) that ceased at 587.5 °C [39]. The weight loss was due to potassium (K) chain fragmentation/decomposition with early oxidation of the samples. The samples indicated thermal stability.

Process factors influence on TFC performance

Impact of dosage on particle removal efficiency

Figure 10 shows initial efficiency of 4 % at 0.5 g/L. This progressively increased to maximum at 46.58 % for 2 g/L, after which it decreased to 6 % at 5 g/L. The efficiency increase resulted from incremental provision of TFC +ve charges that progressively destabilize the PE −ve charges as dosage increased from 0.5 to 2 g/L. Furthermore, the decrease observed after 2 g/L arose from sustained re-stabilization due to oversupply of +ve charges after 2 g/L, up to 5 g/L. At 2 g/L, there was quantitative equilibrium

between both charged species to obtain the optimum performance. Thus, 2 g/L was adopted for the evaluation of influence of pH on particle removal reported in "Impact of pH on particle removal efficiency".

Impact of pH on particle removal efficiency

Figure 11 shows an efficiency profile that alternatively decreased and increased as the pH reduced from 9 to 2. The efficiency increase for pH ranges 3–2 and 8–5 was due to progressive proton donation. Conversely, efficiency suppression for pH ranges 9–8 and 5–3 could be linked to +ve and −ve species-propelled charge reversal, respectively.

Fig. 8 Graph of: **a** DSC and
b TGA of *Tympanotonos
fuscatus* coagulant
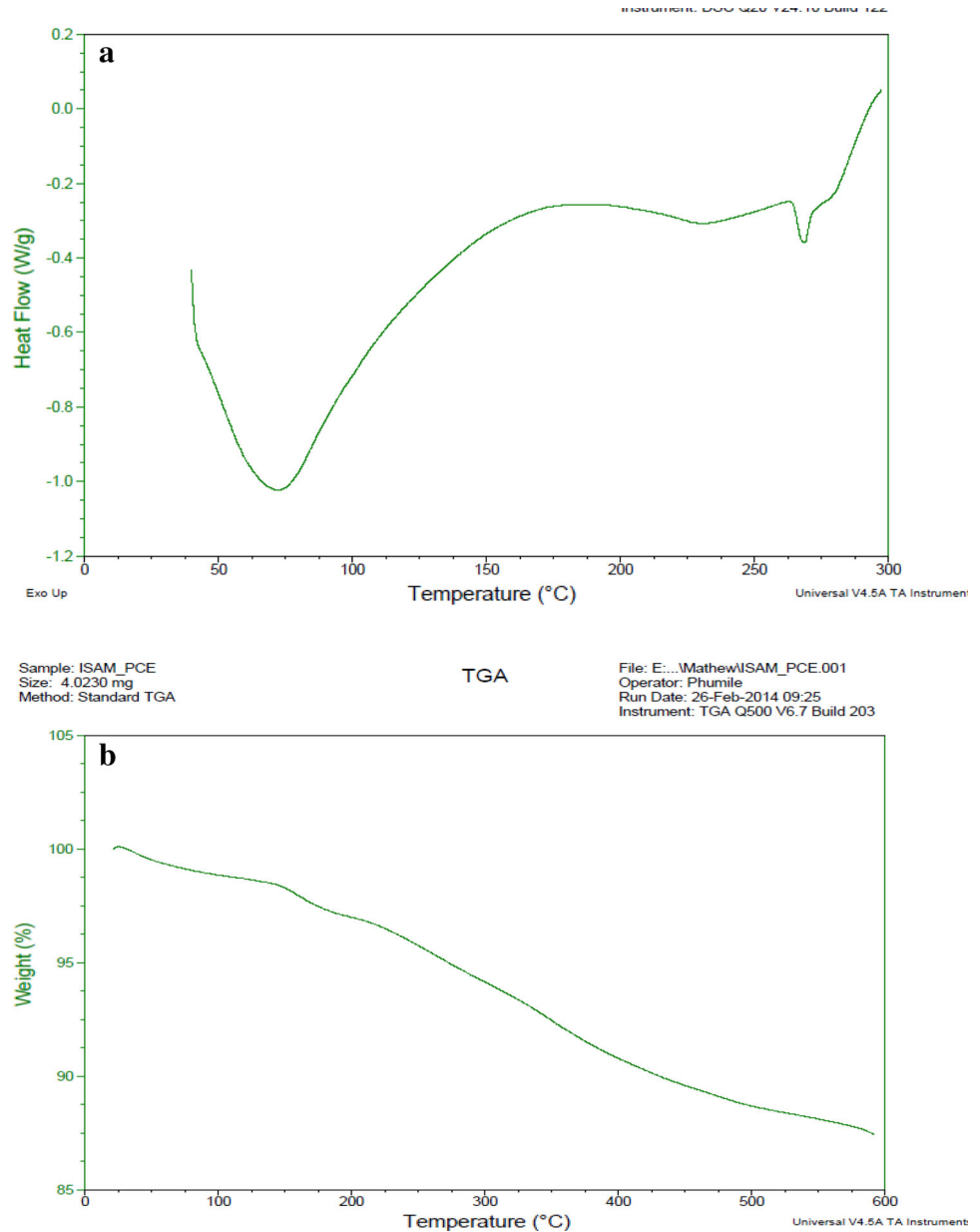
The charge reversal led to re-stabilization and coagulation recession. The peak efficiency at 97 % for pH 5 denotes a regime of equilibrated donation of ions and counter-ions engaged in the perikinetic aggregations.
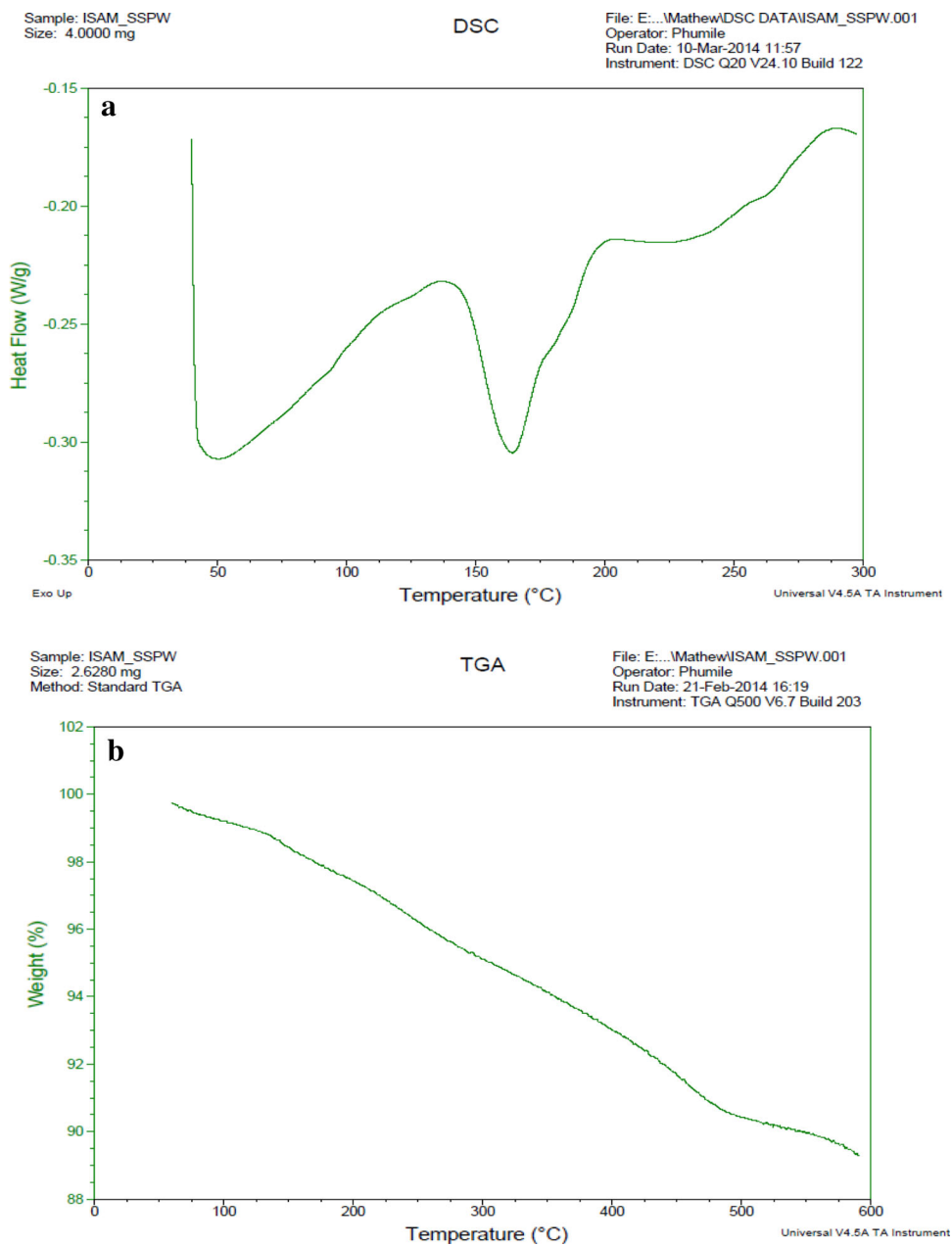
Temporal variation of efficiency

Figure 12 depicts the temporal variation of efficiency with reference to 2 g/L TFC. It shows time-lined increment in efficiency until 20 min, from which efficiency growth becomes negligible. At 20 min, equilibrium was achieved. Between 0 and 20 min, particle aggregation and gravity settling occurred as destabilization or enmeshment effectively took control of the flocculation.
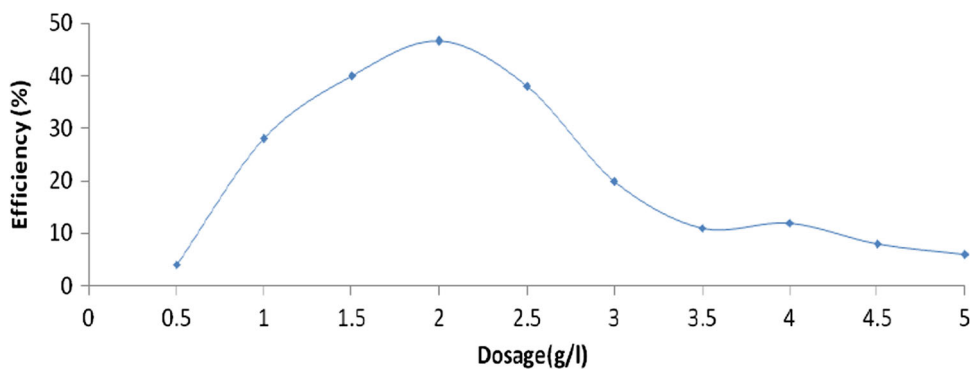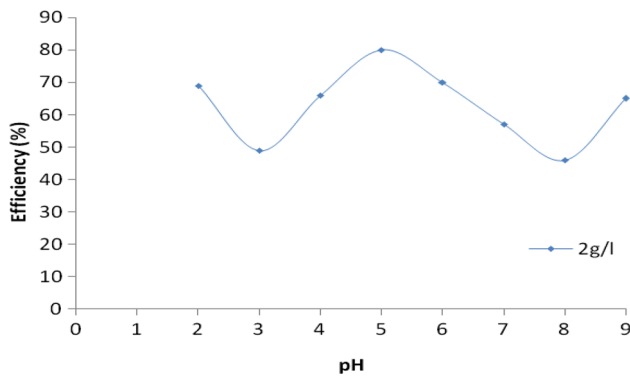
Coag-flocculation kinetics

Table 4 shows the kinetic parameter values for 2.0 g/L and pH 5. K_m was derived from the slope of Eq. (16). K_m takes into account the coagulation and flocculation regimes involved in the aggregation for second-order predominated process. In this case, for higher α to be actualized, a lower is obtained. The value of α is in consonance with earlier reports on Brownian coagulation [20, 28]. α is best maintained between 1 and 2 for effective performance. When variation in K_R is negligible, ε_p directly relates to $2K_m = \beta_{BR}$. In this case, high ε_p results in high kinetic energy to overcome the zeta potential. Low zeta potential ensures recession or total double-layer collapse to actualize

Fig. 9 Graph of: **a** DSC and
b TGA of settled sludge after
treatment

Sample: ISAM_SSPW
Size: 4.0000 mg
DSC
File: E:...\Mathew\DSC DATA\ISAM_SSPW.001
Operator: Phumile
Run Date: 10-Mar-2014 11:57
Instrument: DSC Q20 V24.10 Build 122

Exo Up   Universal V4.5A TA Instrument

Sample: ISAM_SSPW
Size: 2.6280 mg
Method: Standard TGA
TGA
File: E:...\Mathew\ISAM_SSPW.001
Operator: Phumile
Run Date: 21-Feb-2014 16:19
Instrument: TGA Q500 V6.7 Build 203

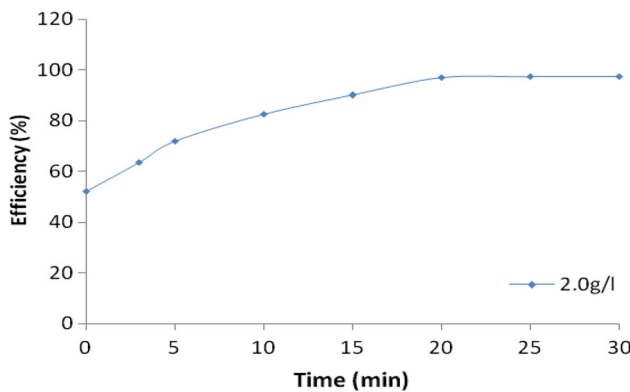Universal V4.5A TA Instrument

Fig. 10 Removal efficiency vs
dosage for *Tympanotonos
fuscatus* coagulant in paint
effluent

Fig. 11 Optimal condition of pH on particle removal efficiency at 2 g/L

Fig. 12 Variation of efficiency with time at 2 g/L and pH 5

Table 4 Coagulation kinetic parameters (pH 5 and 2 g/L)

Parameter	Value
K_m (L g^{-1} s^{-1})	5.0E–5
$\frac{1}{N_0}$ (L g^{-1})	0.0019
N_0 (g L^{-1})	526.30
R^2	0.8576
$\tau_{1/2}$ (s)	76
K_R (g^2 s^{-1})	2.55E–10
β_{BR} (L g^{-1} s^{-1})	1.0E–40
$\mathring{a}_p$ (L^3 g^{-3})	1958
D_p (g^{2}m^{-1}s^{-1})	3.54E–05
Ü	2

low $\tau_{1/2}$ in favor of high rate of coagulation. The model rate equation at which viable flocs materialize at 2 g/L and pH 5 is displayed in Table 5. The discrepancies occurring in kinetic parameters could be attributed to interplay between van der Waals and hydrodynamic forces, which reduces by factor of 2 the correlation between experimental and theoretical values [19, 24, 40, 41].

Table 5 Rate equation for *Tympanotonos fuscatus* coagulant in PE

Dosage (g/L)	Rate equation $(-r)$
2	5.00E$-$05Nt^2

Table 6 Statistical analysis

	Av	SD	RMSE	SSE	RE
Eff. vs dosage	21.36	14.88			
Eff. vs pH	62.75	10.65			
EFF. vs time	81.46	16.2	0.0352	0.2302	0.0287

Eff. efficiency

Process variables statistics

The standard deviation (SD) and statistical error analyses with respect to Figs. 10–12 and Fig. 12, respectively, are represented in Table 6. The SD values (14.88, 10.65, 16.2) shown in Table 2 indicate relative volatility in the efficiency profiles of Figs. 10–12 and Fig. 12. The volatility is amply supported by the graph lines and this was due to alternate swings between protonation and de-protonation of the effluent fluid as pH, time and dosage varied. The relative statistical distance of the SD values from zero indicated profound effect of time, dosage and pH and their capacity to set up aggregation and charge reversal on the process. The results of error analyses with respect to Fig. 12 are shown in Table 6 as RMSE (0.0352), SSE (0.2302), and RE (0.0287). These results indicate how absolute the kinetic data fit the model. The lower the values of RMSE, SSE and RE, the better the fit. Considering the relatively low values of RMSE, Re and SSE, it can be said that the model is reasonably accurate.

Conclusion

In this work, the coagulation–flocculation process was initiated as a pretreatment method to remove particle load from paint effluent (PE) using *Tympanotonos fuscatus* coagulant (TFC). At optimum condition, TFC was found to be an effective bio-coagulant in the pretreatment of paint effluent with particle removal efficiency of 97 % at dosage of 2 g/L and pH of 5. Dosage and pH had significant influence on the performance of TFC. Rate constant of 5.0E$-$5 L g^{-1}s^{-1} was obtained for a period of 76 s. DSC and TGA depicted a thermally stable TFC. SSAT showed a eutectic characteristic, indicating inhomogeneous composition of after treatment sludge (SSAT). The variation in

chemical compositions of TFC and SSAT indicated the ability of the TFC to uptake pollutants away from the paint effluent. This work demonstrates that TFC has potential for application as a coagulant, and could be extended to other effluents.

References

1. Akyol, A.: Treatment of paint manufacturing wastewater by electrocoagulation. Desalination **285**, 91–99 (2012)
2. Karthik, M., Dafale, N., Pathe, P., Nandy, T.: Biodegradability enhancement of purified terephthalic acid wastewater by coagulation–flocculation process as pretreatment. J. Hazard. Mater. **154**, 721–730 (2008)
3. Menkiti, M.C., Nnaji, P.C., Nwoye, C.I., Onukwuli, O.D.: Coagulation–flocculation kinetics and functional parameters response of mucuna seed coagulant of pH variation in organic rich coal effluent medium. J. Miner. Mater. Charact. Eng. **9**(2), 89–103 (2010)
4. Menkiti, M.C., Ndaji, C.R., Ezemagu, I.G., Oyoh, K.B., Menkiti, N.U.: Purification of petroleum produced water by novel afzelia Africana extract via single angle nephlometry. J. Env. Chem. Eng. **3**, 1802–1811 (2015)
5. Gregory, J.: Particles in Water: Properties and Processes. IWA Publishing/CRC Press, London (2006)
6. Wang, J., Chen, Y., Ge, X.W., Yu, H.Q.: Optimization of coagulation–flocculation process for a paper-recycling wastewater treatment using response surface methodology. Colloids Surf. A **302**(1–3), 204–210 (2007)
7. Liew, G., Noor, M.J.M.M., Muyibi, S.A., Fungara, A.M.S., Muhammed, T.A., Iyuke, S.E.: Surface water clarification using *M.* Oleifera seeds. Int. J. Environ. Stud. **63**(2), 211–219 (2006)
8. Barrera-Diaz, C., Linares-Hernandez, I., Roa-Morales, G., Bilyeu, B., Balderes-Hernandez, P.: Removal of biorefractory compounds in industrial wastewater by chemical and electrochemical pretreatments. Ind. Eng. Chem. Res. **48**, 1253–1258 (2009)
9. Miller, S.M., Fugate, E.J., Craver, V.O., Smith, J.A., Zimmerman, J.B.: Towards understanding the efficacy and mechanism of *Opuntia* spp. as a natural coagulant for potential application in water treatment. Environ. Sci. Technol. **42**, 4274–4279 (2008)
10. Crapper, D.R., Krishnan, S.S., Dalton, A.J.: Brain aluminium distribution in alzheimer disease and experimental neurofibrillary degeneration. Science **180**(4085), 511–513 (1973)
11. Ezemagu, G.: Nephlometric study of adsorptive and non-adsorptive components of coagulation of produced water and paint effluent using bioextract. M.Sc Dissertation. Nnamdi Azikiwe University, Awka (2015)
12. Tripathi, P.N., Chaundhuri, N., Bokil, S.D.: Nirmali seed a naturally occurring coagulant. Indian J. Environ. Health **18**(4) (1976)
13. Al-Samawi, A.A., Shokralla, E.M.: An investigation into an indigenous natural coagulants. J. Environ. Sci. Health Part A Environ. Sci. Eng. Toxic Hazard. Subst. Control **8**, 1881–1897 (1996)
14. Menkiti, M.C., Onukwuli, O.D.: Coag-flocculation of mucuna seed coagflocculant (MSC) in coal washery effluent (CWE) using light scattering effects. AICHE J. (2012). doi:10.1002/aic.12665
15. Gunaratna, K.R., Garcia, B., Andersson, S., Dalhammar, G.: Screening and evaluation of natural coagulants for water treatment. Water Sci. Technol. Water Supply **7**(5/6), 19 (2007)
16. *Tympanotonos fuscatus.* http://www.gastropods.com/2/Shell_1612.shtml. Accessed 22 Aug 2015
17. Fernandez, K.: Physiochemical and functional properties of Crawfish Chitosan as affected by different processing protocols. M.Sc Thesis, Dept. of Food Science; Louisiana State University, USA, pp. 1–3, 32–40 (2004)
18. Jamabo, N.A., Chindah, A.C., Alfred, J.F.: Ockiya, length-weight relationship of a Mangrove Prosobranch *Tympanotonos fuscatus* var fuscatus (Linnaeus 1758 from the bonny estuary, Niger Delta, Nigeria). World J. Agric. Sci. **5**(4), 384–388 (2009)
19. Afred-Ockiya, J.F.: Microbial flora of partially processed periwinkles (*Tympanotonos fuscatus*) from local markets in Port Harcourt, Nigeria. Niger. J. Aquat. Sci. **14**, 51–53 (1999)
20. Menkiti, M.C., Nnaji, P.C., Onukwuli, O.D.: Coag-flocculation kinetics and functional parameters response of periwinkle shell coagulant (PSC) to pH variation in organic rich coal effluent medium. Nat. Sci. **7**(6), 1–18 (2009)
21. Verma, S., Prasad, B., Mishra, I.M.: Pretreatment of petrochemical wastewater by coagulation and flocculation and the sludge characteristics. J. Hazard. Mater. **178**, 1055–1064 (2010)
22. Clesceri, L.S., Greenberg, A.E., Eaton, A.D.: Standard Methods for the Examination of Water and Waste Water, 20th edn. APHA, USA (1999)
23. Metcalf and Eddy: Physical unit process, waste water engineering treatment and reuse, 4th edn. Tat-McGraw Hill, New York (2003)
24. Swift, D.L., Friedlander, S.K.: The coagulation of hydrolysis by Brownian motion and laminar shear flow. J. Colloid Sci. **19**, 621 (1964)
25. Jin, Y.: Use of high resolution photographic technique for studying coagulation/flocculation in water treatment. M.SC Thesis, University of Saskatchewan, Saskatoon, Canada, pp. 22–29 (2005)
26. Holthof, H., Egelhaaf, S.U., Borkovec, M., Schurtenberger, P., Sticher, H.: Coagulation rate measurement of colloidal particles by simultaneous static and dynamic light scattering. Langmuir **12**, 5541 (1996)
27. Von Smoluchowski, M.: Versucheiner MathematischenTheorie der Koagulations Kinetic KolloiderLousungen. Z. Phys. Chem. **92**, 129–168 (1917)
28. VanZanten, J.H., Elimelechi, M.: Determination of rate constants by multi angle light scattering. J. Colloid Interface **154**(1), 1–7 (1992)
29. Hunter, R.J.: Introduction to Modern Colloid Science. Oxford University Press, New York (1993), pp. 33–38;289–290
30. (WST) Water Specialist Technology: About coagulation and flocculation. Inf. Bull. USA 1–10 (2003)
31. Santos, E.V., Rocha, J.H.B., Medeiros de Araújo, D., Chianca de Moura, D., Martínez-Huitle, C.A.: Decontamination of produced water containing petroleum hydrocarbons by electrochemical methods: a minireview. Environ. Sci. Pollut. Res. **21**, 8432–8441 (2014)

32. Igunnu, E.T., Chen, G.Z.: Produced water treatment technologies. Int. J. Low Carbon Technol. **9**, 157–177 (2014)

33. Stuart, B.H.: Infrared Spectroscopy: Fundamentals and Application, pp. 71–93. Wiley, USA (2004)

34. Haines, P.J.: The Royal Society of Chemistry, Cambridge (2002)

35. Brukh, R., Mitra, S.: Kinetics of carbon nanotube oxidation. J. Mater. Chem. **17**, 619–623 (2007)

36. Vyazovkin, S.: Thermogravimetric Analysis, Characterization of Materials, 2nd edn, pp. 1–12. Wiley, USA (2012)

37. Ramani, K., Jain, S.D., Mandal, A.B., Sekaran, G.: Microbial induced lipoprotein biosurfactant from slaughterhouse lipid waste and its application to the removal of metal ions from aqueous solution. Colloids Surf. B Biointerfaces **97**, 254–263 (2012)

38. Menkiti, M.C., Aneke, M.C., Ejikeme, P.M., Onukwuli, O.D., Menkiti, N.U.: Adsorptive treatment of brewery effluent using activated *Chrysophyllum albidium* seed shell carbon. SpringerPlus **3**, 213 (2014)

39. Verma, S., Prasad, B., Mishra, I.: Pretreatment of petrochemical wastewater by coagulation and flocculation and the sludge characteristics. J. Hazard. Mater. **178**, 1055–1064 (2010)

40. Holthof, H., Schmitt, A., Barbero, F., Borkovec, M., Vilehez, C., Schurtenberger, P., Hidalgo-Alvarez, R.: Measurement of absolute coagulation rate constants for colloidal particles: comparison of single and multiparticle light scattering techniques. J. Colloid Interface Sci. **192**, 462–470 (1997)

41. Ugonabo, V.I., Menkiti, M.C., Onukwuli, O.D.: Effect of coag-flocculation kinetics on *Telfairia occidentalis* seed coagulant (TOC) in pharmaceutical wastewater. Int. J. Multidisp. Sci. Eng. **9** (2012)